Proceedings of NCFMFP2006
33rd National and 3rd International Conference on Fluid Mechanics and Fluid Power
December 7-9, 2006, IIT Bombay, India

Paper No. NCFMFP2006-1611

SINGLE-PHASE AND TWO-PHASE FLOW PRESSURE DROP ACROSS VARIOUS COMPONENTS OF AHWR FUEL BUNDLE

M.R. Gartia
Reactor Engineering Division
Bhabha Atomic Research Centre
Trombay, Mumbai- 400 085
manas_gartia @ yahoo.co.in

D.S. Pilkhwal
Reactor Engineering Division
Bhabha Atomic Research Centre
Trombay, Mumbai- 400 085
pilkhwal @ barc.gov.in

P.K. Vijayan
Reactor Engineering Division
Bhabha Atomic Research Centre
Trombay, Mumbai- 400 085
vijayanp @ barc.gov.in

D. Saha
Reactor Engineering Division
Bhabha Atomic Research Centre
Trombay, Mumbai- 400 085
dsaha @ barc.gov.in

ABSTRACT

During the evolution of AHWR fuel design, various fuel cluster designs (e.g. 52-rod, 54-rod) with different number of spacers (five and six) were proposed and evaluated experimentally. Experiments were carried out with full scale models to measure the pressure drops across various components under single-phase (water) and two-phase (air-water) flow conditions. The data were analyzed to obtain friction factor, loss coefficients of spacer and tie plates for different flow rates. Using Least-square non-linear regression analysis, correlations have been proposed based on the experimental data. A comparative study of the existing correlations was also done. As experiments have been conducted on two different configurations of fuel clusters, the possible effect of number of rods and number of spacers on the friction factor and loss coefficients have been evaluated.

INTRODUCTION

Pressure drop is an important parameter for design and analysis of many systems and components of AHWR (Advanced Heavy Water Reactor) which is a two-phase natural circulation based reactor. In natural circulation systems, the mass flux and the driving heads are low compared to those of forced circulation systems. Therefore, it is necessary to determine the pressure loss components very accurately. The various components of the fuel bundle are the fuel rods, spacers (to maintain the interspacing between fuel rods), and the tie plates (to hold the fuel pins together at the ends). Due to the complex geometry of these components, experimental investigations are often necessary to determine the pressure drop under single- and two-phase flow conditions. Especially single-phase pressure drop is very important as it is further utilized to calculate the two-phase pressure drop using two-phase friction multiplier concept. During the evolution of AHWR fuel design, various fuel cluster designs (e.g. 52-rod, 54-rod) with different number of spacers (five and six) were proposed and evaluated experimentally.

This paper describes the experimental set up, data generated, method of analysis and the correlations developed in greater details.

NOMENCLATURE

General symbols

D	: diameter, m
f	: friction factor, dimensionless
g	: acceleration due to gravity, m/s^2
K	: loss coefficient, dimensionless
L	: length, m
P	: pressure, N/m^2
Re	: Reynolds number, dimensionless
v	: specific volume, m^3/kg
V	: velocity, m/s
x	: quality, dimensionless
Z	: elevation, m

Greek Symbols

Δ	: difference
μ	: dynamic viscosity, N s/m^2
ρ	: density, kg/m^3

Subscripts

a, b	: point, location
fb	: fuel bundle
btp	: bottom tie plate assembly
c	: cold (corresponds to impulse line temperature)
cc	: coolant channel
g	: gas (air)
l	: liquid
loss	: loss
m	: measured
sp	: spacer
tot	: total
ttp	: top tie plate assembly
tp	: two-phase

2. EXPERIMENTAL SET-UP AND INSTRUMENTATION

2.1 Description of the Test Facility

Figure 1 shows a schematic diagram of the low pressure flow test facility (FTF). The FTF has the flexibility to connect any test section between the flanges of the suction and discharge headers of the pumps. Two centrifugal pumps in parallel (only one is shown in Fig. 1), with the flexibility to operate either one or both are provided to circulate the flow through the loop. The test section flow can be adjusted to the required value with the help of control valves at the inlet and outlet. Demineralised water was used as the working fluid. Because of closed loop operation, the water gets heated up due to the energy input by the pumps. A cooler was provided to maintain the loop temperature at the required value. Eight differential pressure transmitters (DPTs) were used to measure the pressure drop across the different components of the fuel bundle as shown in Fig. 2. A calibrated orifice meter was used to measure the water flow through the test section. Compressed air was injected at the bottom of the vertical test section. Three parallel rotameters of different ranges were connected to common headers in compressed line to measure the air flow rate. The air flow rate was varied with the help of valves put at the inlet or outlet of these rotameters. The maximum error in water flow rate and pressure drop measurement were $\pm$2% and $\pm$1% respectively. The error in air flow rate measurement was of the order of $\pm$2%. The locations of the pressure taps and the instruments used were decided based on the requirements of the particular test.

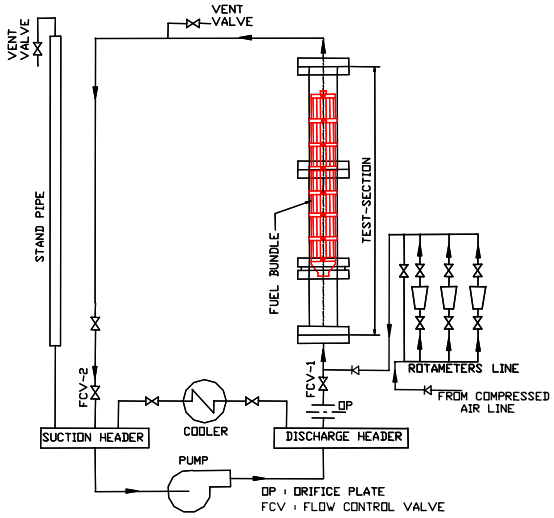

Fig. 1: Schematic of the flow test facility

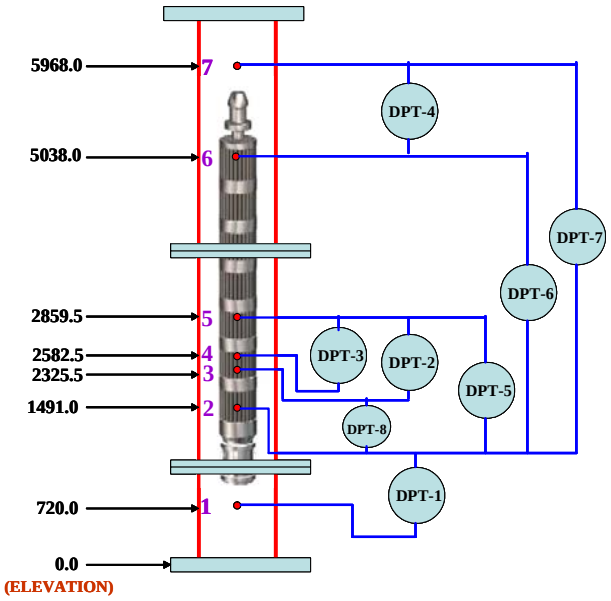

Fig. 2: Test Section and Instrumentation for Fuel Bundle Pressure Drop Experiment

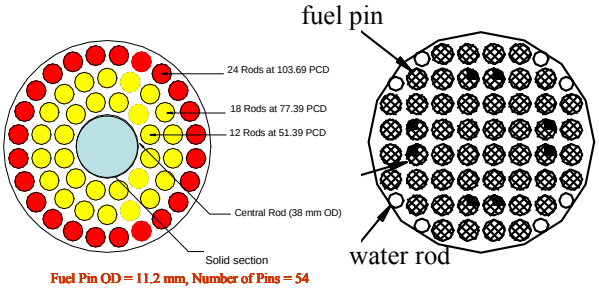

54-rod bundle **52-rod bundle**

Fig. 3: Cross-section of different fuel bundle

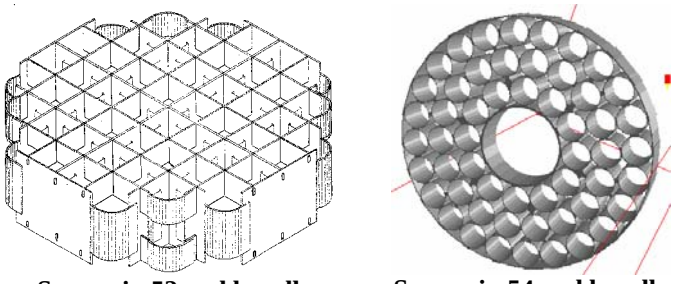

Spacer in 52-rod bundle **Spacer in 54-rod bundle**

Fig. 4: Shape of spacers used in different fuel bundle

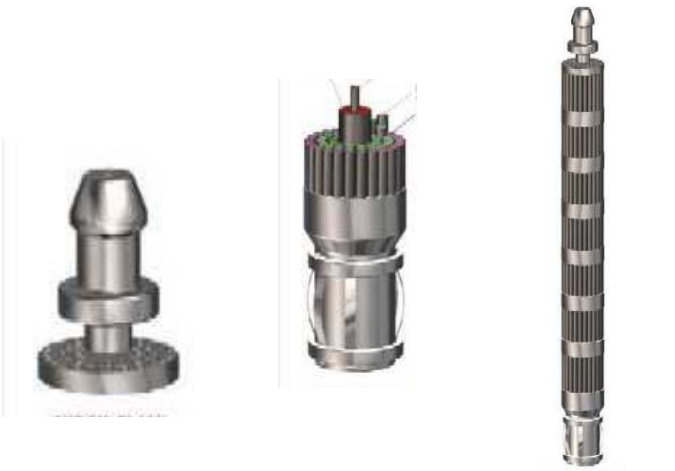

Top tie plate assembly | Bottom tie plate assembly | Complete fuel bundle assembly

Fig. 5: Different components of fuel bundle assembly

2.2 Description of the Test Bundle

The geometric details of 54-rod bundle are shown in Table 1. Figure 3 shows the cross-sectional view of different fuel assembly. The spacers used in 52-rod bundle assembly and 54-rod bundle assembly are shown in Fig 4. Figure 5 shows the bottom tie plate assembly, the top tie plate assembly and 3-dimensional view of a complete fuel assembly.

2.3 Experimental Conditions and Test Procedure

The experimental data were generated at low temperatures (35-37 ^{o}C) covering an air flow range of 160 lpm to 1680 lpm and a water flow range of 350 lpm to 700 lpm. This corresponds to a bundle Reynolds number range of approximately 10,000 to 90,000.

Prior to conducting the experiments, the loop was filled and vented as per standard practice at ambient temperature. The different instruments were calibrated and adjusted for any zero error. The pressure drop measurements were carried out first by increasing the air flow rate from a minimum to maximum value in steps and then decreasing it back to minimum flow rate in steps and in order to check the repeatability, again by increasing to maximum flow rate in steps, while maintaining the water flow rate constant. The same procedure was used for the pressure drop measurements at other water flow rates.

Table-1: Comparison of the geometric details of 52-rod cluster and 54-rod cluster.

	52-rod Cluster	54-rod Cluster
No. of rods	52	54
Rod diameter	11.2 mm	11.2 mm
Channel I.D.	120 mm	120 mm
Flow area	5933.32 mm^2	4855.52 mm^2
Equivalent diameter	10.03 mm	8.105 mm
No. of spacers	5, 6	6
Spacer projected area	1431.94 mm^2	1262.44 mm^2
% Spacer Blockage	24.1	26.0
Height of spacer	48 mm	15 mm
Height of BTP assembly	260 mm	280 mm
Height of TTP assembly	125 mm	220 mm
Distance between two fuel spacers	650 mm (5 sp) 550 mm (6 sp)	540 mm
Length of bundle	3.757 m	3.757 m
Height of 1st Spacer from the top of BTP	541 mm	560 mm

3. METHOD OF ANALYSIS FOR PRESSURE DROP DATA

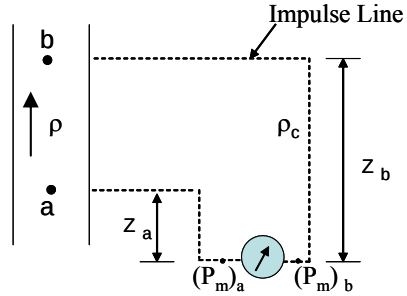

Fig. 6: Arrangement of DPTs in the experimental loop

The pressure drop between any two points 'a' and 'b' (Fig. 6) is given by

$$P_a + \frac{\rho V_a^2}{2} + \rho g Z_a = P_b + \frac{\rho V_b^2}{2} + \rho g Z_b + \Delta P_{loss} \quad (1)$$

ΔP_{loss} is the total pressure drop in segment a-b. Simplifying the above equation we get;

$$P_a - P_b = \frac{\rho (V_b^2 - V_a^2)}{2} + \rho g (Z_b - Z_a) + \Delta P_{loss} \quad (2)$$

If the impulse lines are at a temperature (density, ρ_c) different than that of the flowing fluid temperature then the pressure drop across 'a' and 'b' will be given by

$$P_a - P_b = \rho_c\, g\,(Z_b - Z_a) + (\Delta P_m)_{a\text{-}b} \qquad (3)$$

$(\Delta P_m)_{a\text{-}b}$ is the pressure drop measured by the DPT across 'a' and 'b'. Therefore the total pressure drop across 'a' and 'b' can be given by

$$\Delta P_{loss} = (\Delta P_m)_{a\text{-}b} - (\rho - \rho_c)\, g\,(Z_b - Z_a) - \frac{\rho\,(V_b^2 - V_a^2)}{2} \qquad (4)$$

3.1 For Free Fuel Bundle

Pressure drop across the free length of fuel bundle (segment 3-4) was measured by the difference in reading between DPT-2 and DPT-3 using pressure taps 3, 4 and 5. The pressure loss across the fuel bundle ΔP_{fb} can be given by;

$$\Delta P_{fb} = (\Delta P_m)_{3\text{-}4} - (\rho - \rho_c)\, g\,(Z_4 - Z_3) \qquad (5)$$

The friction factor, f_{fb}, is calculated based on the fuel bundle velocity, V_{fb}, as follows;

$$f_{fb} = \frac{2D}{L}\,\frac{\Delta P_{fb}}{\rho\, V_{fb}^2} \qquad (6)$$

3.2 For BTP Assembly

Pressure taps 1 and 2 were used to measure the pressure drop across the bottom tie plate assembly, with the help of DPT-1 (see Fig. 2). The pressure drop across bottom tie plate assembly, ΔP_{btp}, can be given by;

$$\Delta P_{btp} = (\Delta P_m)_{1\text{-}2} - (\rho - \rho_c)\, g\,(Z_2 - Z_1) - \frac{\rho\,(V_2^2 - V_1^2)}{2} - \Delta P_{cc} - (\Delta P_{fb})_{1-2} \qquad (7)$$

where ΔP_{cc} is the friction pressure drop in the coolant channel portion between pressure tap 1 and to the entry to the divergent section. The ΔP_{fb} is the friction pressure drop in the fuel bundle length after the BTP to pressure tap 2.
The loss coefficient across the bottom tie plate assembly, K_{btp} is calculated based on the fuel bundle velocity, V_{fb}, as follows;

$$K_{btp} = \frac{2.\,\Delta P_{btp}}{\rho\, V_{fb}^2} \qquad (8)$$

3.3 For Fuel Spacer

The pressure drop across six fuel spacers between pressure taps 2 and 6, ΔP_{sp}, can be given by;

$$\Delta P_{sp} = (\Delta P_m)_{2\text{-}6} - (\rho - \rho_c)\, g\,(Z_6 - Z_2) - (\Delta P_{fb})_{2-6} \qquad (9)$$

The loss coefficient across a single fuel spacer, K_{sp}, is calculated as follows;

$$K_{sp} = \frac{1}{6}\left(\frac{2.\,\Delta P_{sp}}{\rho\, V_{fb}^2}\right) = \frac{\Delta P_{sp}}{3\rho\, V_{fb}^2} \qquad (10)$$

3.4 For TTP assembly

Pressure taps 6 and 7 were used to measure the pressure drop across the top tie plate assembly, with the help of DPT-4. The pressure drop across top tie plate assembly, ΔP_{ttp}, can be given by;

$$\Delta P_{ttp} = (\Delta P_m)_{6-7} - (\rho - \rho_c) g (z_7 - z_6) - \frac{\rho\left(V_7^2 - V_6^2\right)}{2} - \Delta P_{cc} - (\Delta P_{fb})_{6-7} \qquad (11)$$

The loss coefficient across the top tie plate assembly, K_{ttp}, is calculated as follows;

$$K_{ttp} = \frac{2.\,\Delta P_{ttp}}{\rho\, V_{fb}^2} \qquad (12)$$

3.5 For Total Pressure Drop

The total pressure drop across the fuel assembly was measured with DPT-1 and DPT-7. The total pressure drop across fuel assembly, ΔP_{tot}, can be given by;

$$\Delta P_{tot} = (\Delta P_m)_{1\text{-}7} - (\rho - \rho_c)\, g\,(Z_7 - Z_1) - \Delta P_{cc} \qquad (13)$$

Where $(\Delta P_m)_{1-7} = (\Delta P_m)_{1-2} + (\Delta P_m)_{2-7}$

The total loss coefficient across the fuel assembly, K_{tot}, is calculated as follows;

$$K_{tot} = \frac{2.\,\Delta P_{tot}}{\rho\, V_{fb}^2} \qquad (14)$$

3.6 Different Models Used

A list of single-phase friction factor correlations used in the present report for comparison with experimental data is given in Table 2. The uncertainty in the experiment has also been estimated. Based on the methodology given by Moffat (1988) and as described by Gartia et al. (2006), the estimated uncertainty in the calculated friction factor is $\pm$ 3.5%.

Table-2: Typical existing single-phase friction factor correlations selected for comparison

Reference	Geometry	Re	Correlation for the friction factor
Blasius (1913)	pipes	3,000~100,000	$f = 0.316\,\mathrm{Re}^{-0.25}$
Grillo and Marinelli (1970)	4 x 4 array	10,000~300,000	$f = 0.1626\,\mathrm{Re}^{-0.2}$
Pilkhwal et al. (2001)	52-rod bundle	7,900~79,000	$f = 0.5529\,\mathrm{Re}^{-0.30205}$
Rehme (1973)	7~37 rod bundle	2,000~250,000	$f = \frac{64}{\mathrm{Re}} + \frac{0.0816}{\mathrm{Re}^{0.133}}$
Rehme (Modified)	54-rod bundle	10,000~35,000	$f = \frac{64}{\mathrm{Re}} + \frac{0.0816}{\mathrm{Re}^{0.163}}$
Snoek and Ahmad (1984)	37-rod bundle	108,000~418,000	$f = 0.05052\,\mathrm{Re}^{-0.05719}$
Vijayan et al. (1999)	37-rod bundle	10,000~500,000	$f = 0.236\,\mathrm{Re}^{-0.17}$

Table 3: List of Correlations Developed for 52- and 54-rod Bundles

Components		**Single-Phase**		**Two-Phase**	
		52-rod Bundle	54-rod Bundle	52-rod Bundle	54-rod Bundle
Bundle	5 Sp	$f_{bl} = 0.1496\,\mathrm{Re}^{-0.19877}$	$f_{bl} = 3.08055\,\mathrm{Re}^{-0.50653}$	$(f_{bl})_{tp} = 590.838\,\mathrm{Re}^{-0.99173}$	$(f_{bl})_{tp} = (f_{bl})_{1\phi} * 3.784\left(\frac{x}{1-x}\right)^{0.0184} * \left(\frac{\rho_l - \rho_g}{\rho_l}\right)^{800.2865} * \left(\frac{\mu_l - \mu_g}{\mu_l}\right)^{0.2}$
	6 Sp	$f_{bl} = 0.5529\,\mathrm{Re}^{-0.30205}$			
Spacer	5 Sp	$K_{sp} = 86.293\,\mathrm{Re}^{-0.36823}$	$K_{sp} = 11.208\,\mathrm{Re}^{-0.14326}$	$K_{sp} = 8.8206\,\mathrm{Re}_{tp}^{-0.21142}$	$K_{sp} = 8377.768\,\mathrm{Re}_{tp}^{-0.80179}$
	6 Sp	$K_{sp} = 51.855\,\mathrm{Re}^{-0.35114}$			
BTP	5 Sp	$K_{btp} = 5.414\,\mathrm{Re}^{-0.07102}$	$K_{btp} = 9.974\,\mathrm{Re}^{-0.13667}$	$K_{btp} = 620.3227\,\mathrm{Re}_{tp}^{-0.58685}$	$K_{btp} = 12504.63\,\mathrm{Re}_{tp}^{-0.84075}$
	6 Sp	$K_{btp} = 8.303\,\mathrm{Re}^{-0.08677}$			
TTP	5 Sp	$K_{ttp} = 6.357\,\mathrm{Re}^{-0.0186}$	$K_{ttp} = 4.758\,\mathrm{Re}^{-0.05393}$	$K_{ttp} = 77.3296\,\mathrm{Re}_{tp}^{-0.29085}$	$K_{ttp} = 147.0722\,\mathrm{Re}_{tp}^{-0.37825}$
	6 Sp	$K_{ttp} = 9.007\,\mathrm{Re}^{-0.07987}$			
Total loss Across Bundle		$K_{tot} = 239.813\,\mathrm{Re}^{-0.22044}$	$K_{tot} = 850.75\,\mathrm{Re}^{-0.31964}$	$K_{tot} = 2968.52\,\mathrm{Re}_{tp}^{-0.48679}$	$K_{tot} = 34334.978\,\mathrm{Re}_{tp}^{-0.66982}$

4. RESULTS AND DISCUSSION

Figure 7 shows the effect of number of spacers on the total loss coefficient. The total loss coefficient across the bundle for 52-rod bundle assembly with 6-spacer configuration is higher than that of same geometry with 5-spacer configuration as expected.

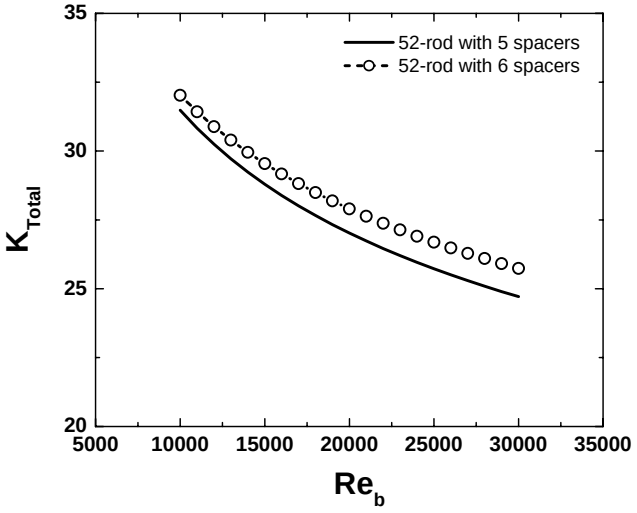

Fig.7: Effect of number of spacers on total loss coefficient

Figure 8(a) shows the variation of spacer loss coefficient with bundle Reynolds number in 52-rod bundle with 6 spacers along with the uncertainties involved in the experimental data. However, the spacer loss coefficient for 52-rod bundle with 5 spacer is higher than that of 52-rod with 6-spacer as shown in Fig. 8(b). The distance between two spacers for 5-spacer configuration is more than that of 6-spacer configuration. Hence the flow will be more regular after emerging from spacer in 5-spacer configuration than in 6-spacer configuration. Also, the geometry and flow areas in these two sets of spacers are the same and hence the turbulence flow pattern after the spacers can be assumed to be the same. So, in 52-rod with 5-spacer case, the pressure drop across the spacer will be between a turbulent flow at the top and regular flow at the bottom; whereas for 52-rod with 6-spacer, the spacer pressure drop is calculated when the spacer is between two turbulent flow regime at the top as well as at the bottom. Because of this reason the pressure drops across a single spacer for 52-rod with 5-spacer configuration is higher than that of 6-spacer configuration.

Figure 9 shows the combined effect of spacer shapes and number of rods on the total loss coefficient across the bundle. The 52-rod cluster uses a honey-comb type spacer while the 54-rod cluster uses a ring type spacer as shown in Fig. 4. Since there will be more eddies formation in a honey-comb structure than a ring type spacer and because of higher number of bare rods, the total pressure drop across a 54-rod cluster will be higher than that of 52-rod cluster and hence higher total loss coefficient for 54-rod cluster as shown in Fig. 9.

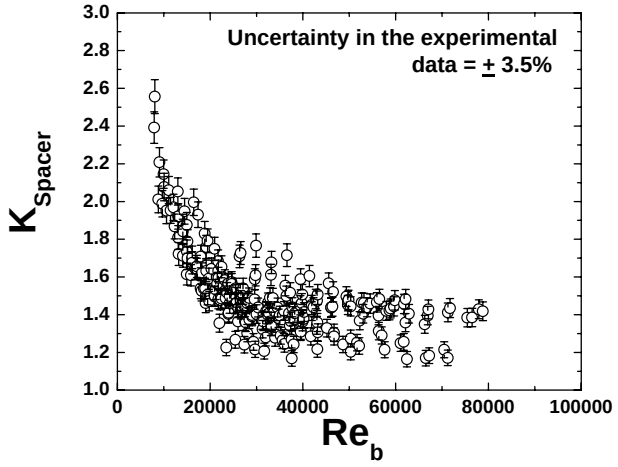

Fig. 8(a): Spacer loss coefficient for 52-rod with 6 spacer along with the uncertainty bar

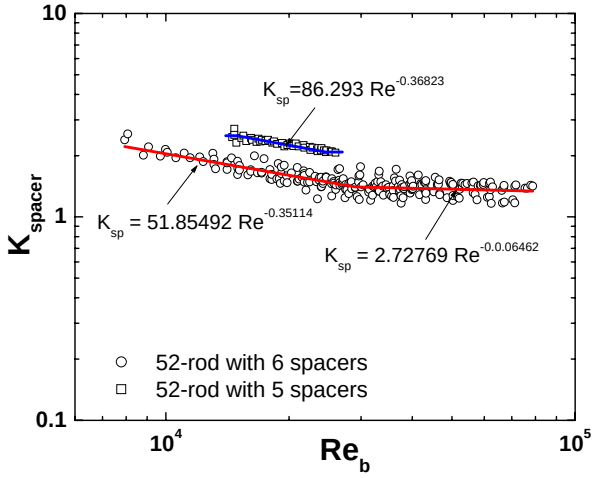

Fig. 8(b): Effect of number of spacers on spacer loss coefficient

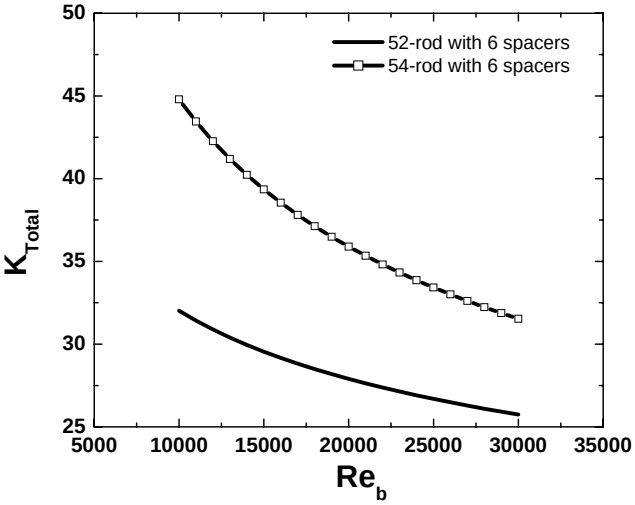

Fig. 9: Effect of shape and flow area of spacers on total loss coefficient

Unlike the circular tube case, in which an obvious transition from laminar to turbulent flow conditions occurs around Reynolds number equal to 2100, in rod bundles the transition from laminar conditions occur as early as 400 to 1000 and the transition to turbulent conditions occurs later around 12000 to 20000 (Cheng and Todreas (1986)). These transitions depend upon the P/D (pitch-to-diameter ratio) of the bundle. The effect of P/D on the transition Reynolds number is shown in Fig. 10.

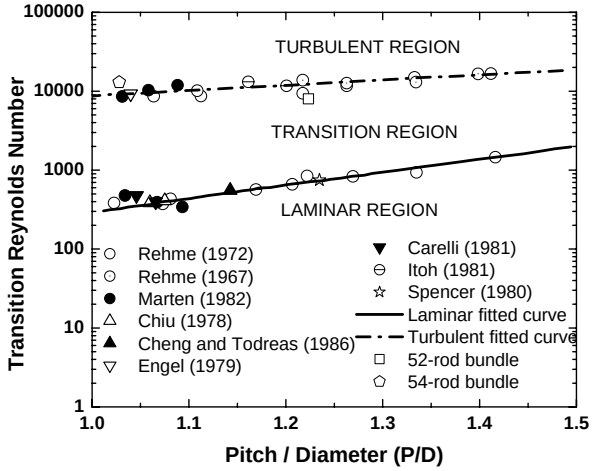

Fig. 10: Effect of P/D ratio on the Reynolds number at which flow transitions occur

It is clear from the figure that with the increase in P/D ratio the transition to turbulent flow occurs at a higher Reynolds number. That is, when the flow in a rod bundle with lower pitch has just crossed to turbulent region, for the same Reynolds number the flow will be still in transition region in a rod bundle with higher pitch. Therefore, for the same Reynolds number, a rod bundle with higher pitch will be having higher friction factor. In fact the variation of bundle friction factor with Reynolds number from five different bundles with different P/D was compared in Fig. 11. It showed that bundle with highest P/D is having the highest bundle friction factor.

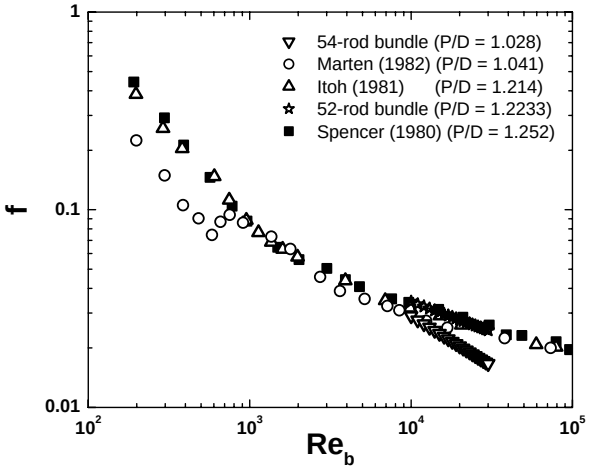

Fig. 11: Effect of P/D ratio on the bundle friction factor

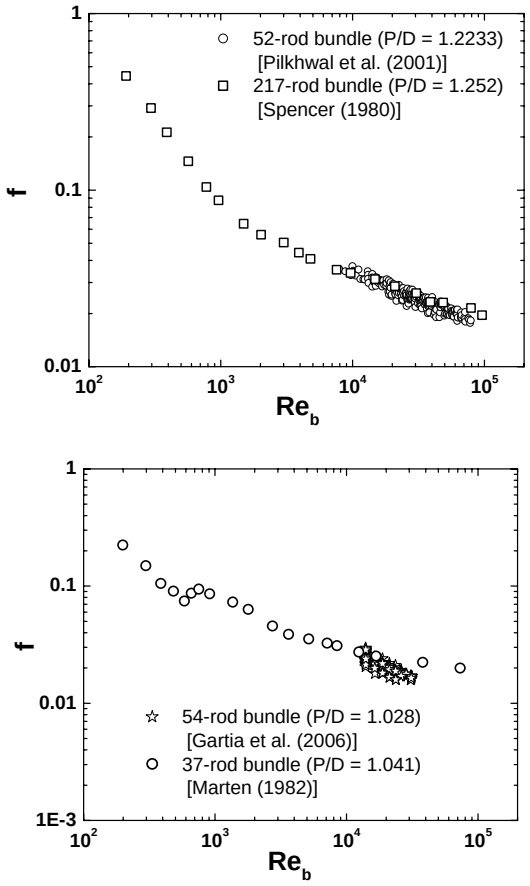

Fig. 12: Effect of number of bare rods on friction factor

Figure 12 shows how the friction factor depends on the number of rods in a rod bundle. The friction factor increases with increasing number of rods. This effect can be explained by the fact that the influence of the smooth channel wall results in a lower pressure loss. Since rod bundles with only a few rods include a relatively higher part of channel wall with respect to the total wetted perimeter, the total pressure drop is lower.

Figure 13 shows the variation of spacer loss coefficient with Reynolds number for different shapes of spacer. It showed that the loss coefficient for a ring type spacer (as used in 54-rod bundle) is more than that of a honeycomb type spacer (as used in 52-rod bundle) without considering the plugging effect. Whereas after considering the plugging effect, the loss coefficient for the honeycomb type spacer is more than the ring type spacer. This is due to the fact that the chances of flow separation in a honeycomb (grid) type spacer are more than that of a ring type spacer. But by taking into account the relative plugging affect (= projected grid cross section / undisturbed flow section) Rehme (1973) found that at high Reynolds number the loss coefficient in ring-type spacer is more than that of a honeycomb (grid) type spacer which is in agreement with the current finding.

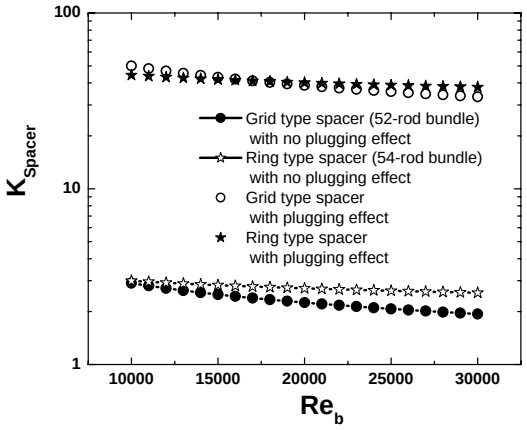

Fig. 13: Effect of shape of spacers on loss coefficient

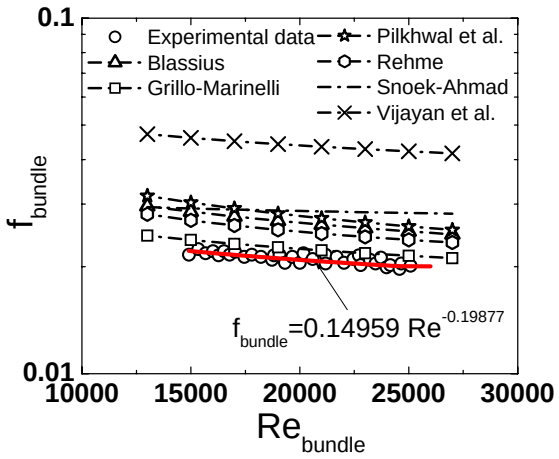

Fig. 14(a): Variation of friction factor for 52-rod bundle assembly with 5 spacers under single-phase

Figure 14a shows the variation of free fuel bundle friction factor with bundle Reynolds number for 52-rod cluster with 5 spacers under single-phase condition. For comparison purpose, the predicted values of friction factors by different models are also plotted in this figure. It is seen that all the correlations are over predicting the friction factor under the present experimental condition. The prediction by Grillo and Marinelli (1970) correlation is the closest of all correlations matched with the experimental data. This may be because Grillo-Marinelli correlation was developed for a 16-rod cluster with square lattice and the 52-rod cluster is arranged in a similar square lattice formation.

Figure 14b, c and d show the variation of spacer loss coefficient, bottom tie plate assembly loss coefficient and top tie plate assembly loss coefficient respectively for 52-rod cluster with 5 spacer configuration under single phase condition.

Figure 15a, b, c and d show the variation of bare bundle friction factor, spacer loss coefficient, bottom tie plate assembly loss coefficient and top tie plate assembly loss coefficient respectively for 52-rod cluster with 5 spacer configurations under two phase condition.

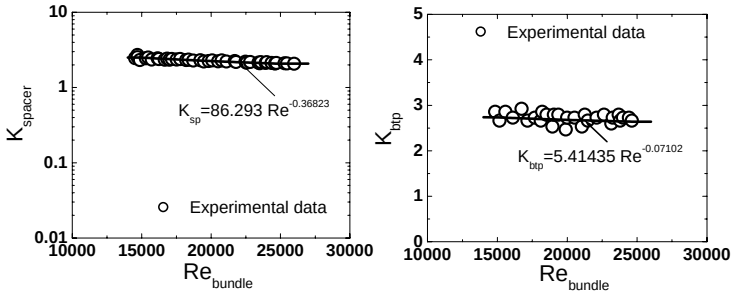

(b) **(c)**

Fig. 14: Variation of (b) Spacer loss coefficient (c) BTP loss coefficient for 52-rod bundle assembly with 5 spacers under single-phase

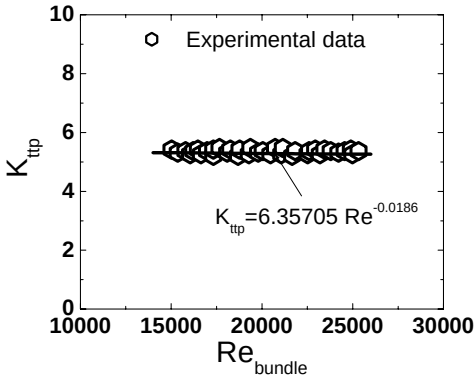

Fig. 14(d): Variation of TTP loss coefficient for 52-rod bundle assembly with 5 spacers under single-phase

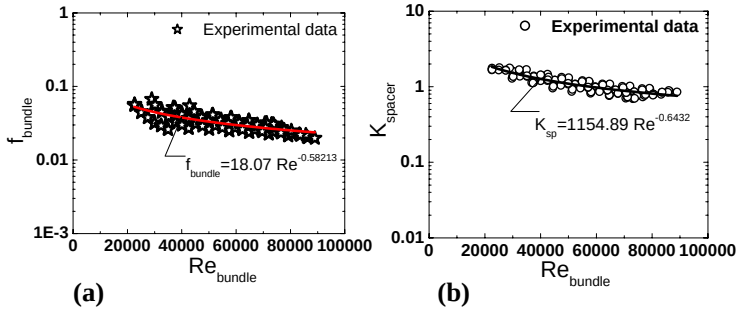

(a) **(b)**

Fig. 15: Variation of (a) friction factor (b) Spacer loss coefficient for 52-rod bundle assembly with 5 spacers under two-phase

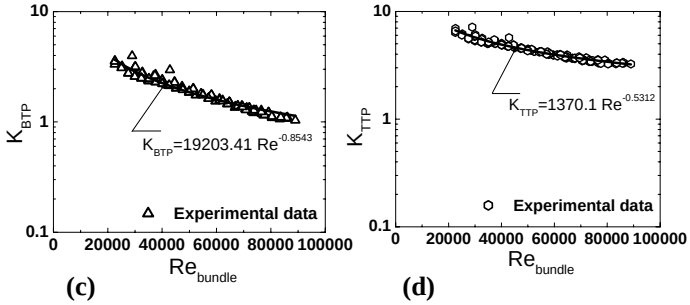

(c) **(d)**

Fig. 15: Variation of (c) BTP loss coefficient and (d) TTP loss coefficient for 52-rod bundle assembly with 5 spacers under two-phase

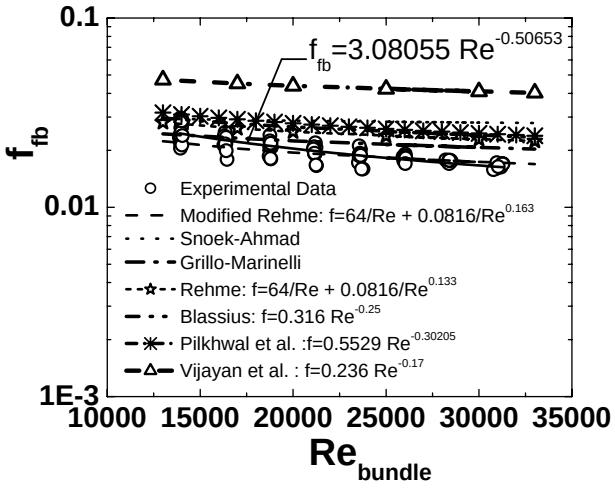

Fig. 16(a): Variation of friction factor for 54-rod bundle assembly with 6 spacers under single-phase

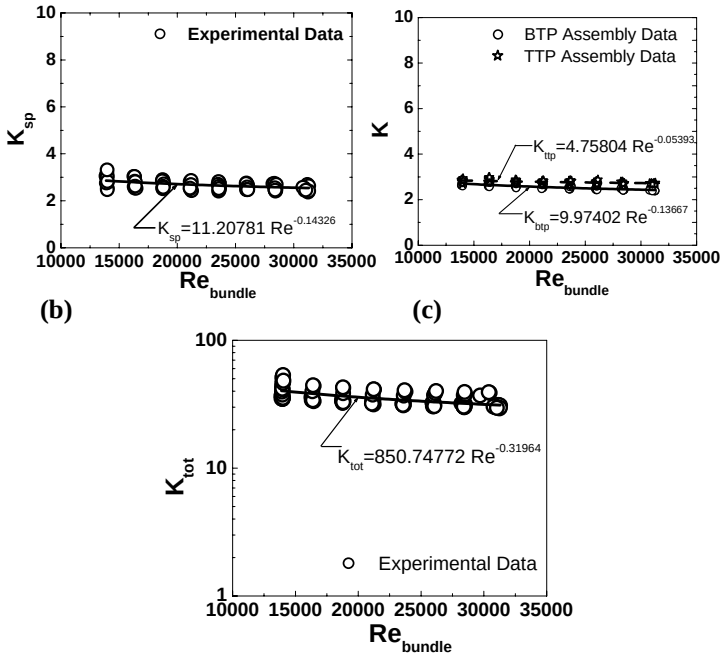

Fig. 16: Variation of (b) Spacer loss coefficient (c) BTP and TTP loss coefficient and (d) Total loss coefficient across bundle for 54-rod bundle assembly with 6 spacers under single-phase

Figure 16a shows the variation of free fuel bundle friction factor with bundle Reynolds number for 54-rod cluster with 6 spacers under single-phase condition. The predicted friction factor was compared with seven different existing friction factor correlations as listed in Table 2. The result of the study showed that the Rehme (1973) model with modification in the exponent of Reynolds number from 0.133 to 0.163 gave good agreement with experimental data in the turbulent flow regime. The variation of loss coefficient for spacer, BTP and TTP assembly and total loss coefficient across the bundle assembly is shown in Fig. 16b, c and d respectively.

Figure 17a, b, c and d show the variation of bare bundle friction factor, spacer loss coefficient, BTP and TTP assembly loss coefficient and total loss coefficient across the fuel bundle assembly respectively for the 54-rod cluster with 6 spacer configurations under two phase condition.

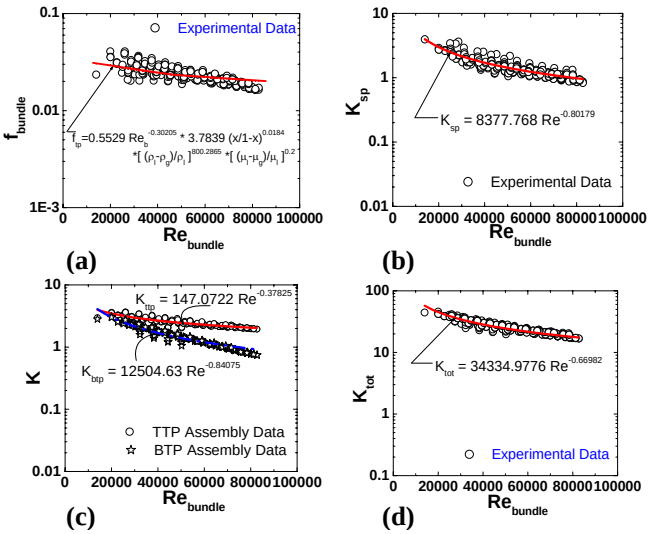

Fig. 17: Variation of (a) friction factor (b) Spacer loss coefficient (c) BTP and TTP loss coefficient and (d) Total loss coefficient across bundle for 54-rod bundle assembly with 6 spacers under two-phase

Similarly Figure 18a, b and c show the variation of bare bundle friction factor, spacer loss coefficient, and BTP and TTP assembly loss coefficient respectively for the 52-rod cluster with 6 spacer configurations under single phase condition.

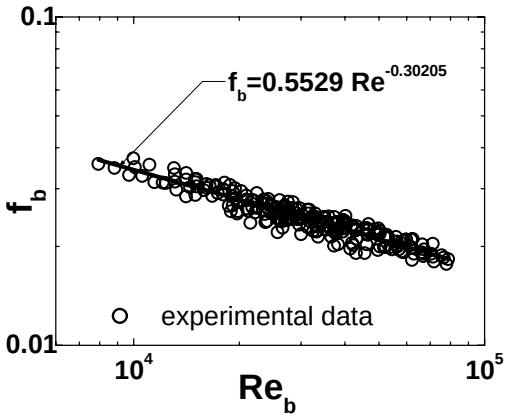

Fig. 18(a): Variation of friction factor for 52-rod bundle assembly with 6 spacers under single-phase

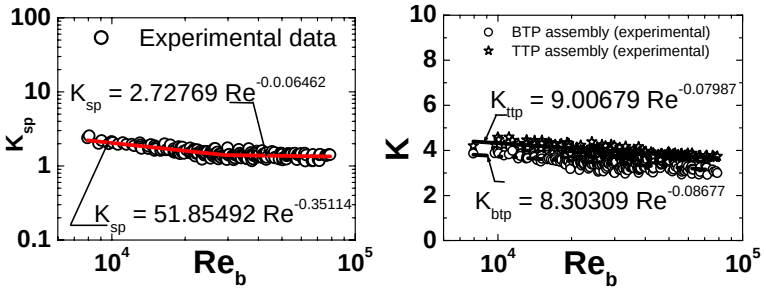

Fig. 18: Variation of (b) Spacer loss coefficient and (c) BTP and TTP loss coefficient for 52-rod bundle assembly with 6 spacers under single-phase

5. CONCLUSIONS

Experiments were carried out to measure the pressure drop across the various components of 52-rod with 5 spacers and 54-rod cluster with 6 spacers under single-phase and two-phase conditions. From the measured values of pressure drop, friction factor for bare bundle, loss coefficients for spacers, tie plate assemblies (TTP and BTP) and total fuel bundle were derived for both single-phase as well as two-phase conditions.

The results showed that the total loss coefficient for 52-rod with 6 spacers is more than that for 52-rod with 5 spacer configuration. In contrast the loss coefficient across a single spacer for 52-rod with 5 spacers is more than that of 52-rod with 6 spacers. Also, the total loss coefficient for 54-rod with 6-spacers is more than that of 52-rod with 6-spacer configuration. The transition Reynolds number depends on the P/D and with the increase in P/D the Reynolds number at which transition occurs also rises. The bundle with a higher P/D will be having higher friction factor than a bundle with lower P/D. For a same P/D, bundle with higher number of rods will be having higher bundle friction factor. The loss coefficient for the ring type spacers is found to be more than that of honeycomb type spacers.

Finally the single phase friction factor for bare bundle was compared with the available models. Grillo and Marinelli correlation was found to be predicting better than the others for 52-rod with 5 spacer. The prediction by Rehme correlation was in good agreement with the experimental data for 54-rod with 6 spacer configuration.

ACKNOWLEDGEMENT

The authors wish to thank the staff of Divisional Workshop, Instrumentation Section and Engineering Facility Section of Reactor Engineering Division for their technical assistance.

REFERENCES

1. Blasius, H., Mitt. Forsch. Geb. Ing.-Wesen, **131,** 1913.
2. Cheng, S.K. and Todreas, N.E., Hydrodynamic models and correlations for bare and wire-wrapped hexagonal rod bundles-bundle friction factors, subchannel friction factors and mixing parameters, Nuclear Engineering and Design, **92**, 227-251, 1986.
3. Chiu, C., Rohsenow, W.M. and Todreas, N.E., Turbulent sweeping flow mixing model for wire wrapped LMBFR assemblies, COO-2245-55TR, Rev. 1, MIT, 1978.
4. Engel, F.C., Markley, R.A. and Bishop A.A., Laminar, transition and turbulent parallel flow pressure drop across wire-wrap-spaced rod bundle, Nuclear Science and Engineering, **69**, 290-296, 1979.
5. Gartia M.R., Pilkhwal D.S., Vijayan P.K. and Saha D., Experimental Investigation of Two-Phase Pressure Drop Across Various Components of Fuel Bundle, 18th National and 7th ISHMT-ASME Heat and Mass Transfer Conference, IIT, Guwahati, India, January 4-6, 2006.
6. Grillo, P. and Marinelli, V., Single and Two-Phase Pressure Drops on a 16-ROD Bundle, Nuclear Applications and Technology, **9**, 682-693, 1970.
7. Marten, K., Yonekawa, S. and Hoffmann, H., Experimental investigation on pressure drop in tightly packed bundles with wire wrapped rods, IAHR Second International Specialists Meeting on Thermal-Hydraulics in LMBFR Rod Bundles, Rome, Sept. 1982.
8. Moffat, Robert J., Describing the uncertainties in experimental results, Experimental Thermal and Fluid Sciences, **1**, 3-17, 1988.
9. Pilkhwal, D.S., Vijayan, P.K., Saha, D. and Sinha, R.K., Experimental Investigation of Pressure Drop across Various Components of AHWR fuel bundle, BARC/2001/I/001, 2001.
10. Rehme, K., Pressure Drop Correlations for Fuel Element Spacers, Nuclear Technology, **17**, 15-23, 1973.
11. Snoek, C.W. and Ahmad, S.Y., A Method of Predicting Pressure Profiles in Horizontal 37 element Clusters, AECL-8065, Chalk River Nuclear Laboratories, Chalk River, Ontario, 1984.
12. Vijayan, P.K., Pilkhwal, D.S., Saha, D. and Venkat Raj, V., Experimental Studies on the Pressure Drop Across the Various Components of a PHWR Fuel Channel, Experimental Thermal and Fluid Science, **20**, 34-44, 1999.